Title

Immunoaffinity-Based Protocol to Enrich Nervous System Cell-, Lung Alveolar Cell-, and Hepatocyte-Derived Extracellular Vesicles From Human Plasma

Journal

Journal of Extracellular Biology, 5(7)

ISSN

2768-2811

Authors

Pierri, Biancamaria

Jackson, Gabriela L

Gololobova, Olesia

et al.

Publication Date

2026-07-01

DOI

10.1002/jex2.70171

Journal of Extracellular Biology

RESEARCH ARTICLE OPEN ACCESS

Immunoaffinity-Based Protocol to Enrich Nervous System Cell-, Lung Alveolar Cell-, and Hepatocyte-Derived Extracellular Vesicles From Human Plasma

Biancamaria Pierri[1] | Gabriela L. Jackson[1] | Olesia Gololobova[2] | Fang Wang[1] | Erez Eitan[3] | Olga Volpert[3] | Vrinda Kalia[1] | Gissette Reyes-Soffer[4] | Louise C. Laurent[5] | Kenneth W. Witwer[2,6] | Andrea A. Baccarelli[7] | Haotian Wu[1]

[1]Department of Environmental Health Sciences, Mailman School of Public Health, Columbia University, New York, New York, USA | [2]Molecular and Comparative Pathobiology and Neurology, The Johns Hopkins University School of Medicine, Baltimore, Maryland, USA | [3]NeuroDex Inc., Boston, Massachusetts, USA | [4]Division of Preventive Medicine and Nutrition, Department of Medicine, Columbia University, New York, New York, USA | [5]Department of Obstetrics, Gynecology, and Reproductive Sciences, University of California San Diego, La Jolla, California, USA | [6]The Richman Family Precision Medicine Center of Excellence in Alzheimer's Disease, The Johns Hopkins University School of Medicine, Baltimore, Maryland, USA | [7]Office of the Dean, Harvard T.H. Chan School of Public Health, Boston, Massachusetts, USA

Correspondence: Biancamaria Pierri (bp2693@cumc.columbia.edu)

Received: 2 December 2025 | **Revised:** 18 June 2026 | **Accepted:** 23 June 2026

Keywords: biomarkers | ELISA | extracellular vesicles | immunoaffinity | liquid biopsy

ABSTRACT

By preserving molecular information inherited from the source cell, extracellular vesicles (EVs) can serve as biomarkers for tissue health or disease, paving the way for liquid biopsy applications. The enrichment of tissue-specific EVs (TS-EVs) from human biofluids can be challenging due to technical and methodological limitations. Here, we use single and sequential immunoaffinity capture workflows to enrich antigen-specific EVs circulating in human blood. We demonstrate the specificity, efficiency, and consistency of our approach for enriching blood plasma EV subpopulations from the nervous system, alveolar cells and hepatocytes. The enriched subpopulations are characterized by canonical EV features and markers, as well as co-localization of tissue-specific and general markers on the surface. We provide a validated workflow to derive multiple EV subpopulations from circulation, leveraging their promise as informative biomarkers of tissue status and enabling liquid biopsy and biomarker discovery.

1 | Introduction

Extracellular vesicles (EVs) are small membrane-delimited molecules naturally secreted by cells and present in biofluids (Raposo and Stoorvogel 2013, Yáñez-Mó et al. 2015). Carrying a heterogeneous cargo of proteins, nucleic acids, lipids and small metabolites, EVs can transport signals and molecules to nearby or distant targets, which can subsequently induce biological responses in recipient cells or remodel the extracellular environment (Gardiner et al. 2016, Kalra et al. 2016). Their extensive role in cell-to-cell communication is essential for various biological processes under normal physiological or pathological conditions (Buzas 2023). In recent decades, EVs have attracted considerable attention for their pivotal role in intercellular communication (Pegtel and Gould 2019), appealing characteristics for liquid biopsy (Kalluri and LeBleu 2020, Yu et al. 2022), and promise for therapeutic delivery (Wiklander et al. 2019). The ongoing debate regarding their biogenesis, characteristics, and nomenclature has led to the development of standardized research guidelines (MISEV-Minimal Information for Studies of Extracellular Vesi-

cles) to harmonize definitions and approaches in the field (Théry et al. 2018, Welsh et al. 2024).

Circulating EVs are emerging as a new frontier in liquid biopsy for clinical research and application, allowing access to organs that cannot be easily biopsied, such as the brain (Yu et al. 2022, Picca et al. 2022). EVs are carriers of tissue-specific clinical biomarkers, reflecting the phenotypic state and molecular profile of the parental cell (Kalluri and LeBleu 2020). Although the majority of EVs in circulation originate from platelets and hematopoietic cells, many other tissues and cell types also contribute EVs to the blood (Li et al. 2020). Such diversity poses a challenge in terms of enrichment and characterization of tissue-specific EVs (TS-EVs).

Immunoaffinity capture methods, leveraging cell-specific surface antigens, enable the enrichment of specific EV subpopulations (Gao et al. 2023, Mondal and Whiteside 2021, Eitan et al. 2023). However, existing research has suffered from the lack of method standardization, even though enrichment and characterization protocols are continuously improving (Gao et al. 2023). The enrichment of EVs derived from different tissues is challenging due to (i) the relative low abundance of each cell type-derived EV in circulation (Li et al. 2020); (ii) the heterogeneity of the surfaceosome, which is the totality of surface molecules of different EV subpopulations; (iii) the topology, stoichiometry, and relative abundance of the targets on the surface of each EV (Zarovni et al. 2025); (iv) and the interaction of surface markers with apolipoproteins or other proteins, affecting their availability to bind antibodies (Hallal et al. 2022). For these reasons, the effectiveness of the immunoaffinity capture approach is primarily contingent upon the accurate identification of cell-specific surface markers, the density of target markers on EVs, the availability of reliable antibodies, and the absence of non-specific interactions (Stam et al. 2021).

The scientific literature reports several examples of immunoaffinity protocols directed to a subpopulation of EVs supposedly originating from a single cell type. Neuronal EVs, for instance, have been explored in the context of neurodegeneration. Many early studies targeted the L1 cell adhesion molecule (L1CAM) (Picca et al. 2022, Gomes and Witwer 2022, Jiang et al. 2020, Kapogiannis 2017, Kapogiannis et al. 2019) while some recent studies used sodium/potassium-transporting ATPase subunit alpha-3 (ATP1A3) (You et al. 2023), or Neurexin-3 (NRXN3) (Ter-Ovanesyan et al. 2024) or a combination of Growth Associated Protein 43 (GAP43) and Neuroligin 3 (NLGN3) (Eitan et al. 2023, Kalia et al. 2025) to specifically enrich neuronal EV from human plasma and investigate potential biomarkers for Alzheimer's disease (AD) and related neurodegenerative conditions. Neuronal EVs have been demonstrated to transfer misfolded proteins (i.e. amyloid-β and α-synuclein), and their cargo has promise as an informative biomarker of cognitive impairment with AD (Pulliam et al. 2019), preclinical AD (Fiandaca et al. 2015), dementia (Winston et al. 2016), or of disease severity for Parkinson's Disease (PD) (Shi et al. 2014). Progress in neuronal EVs illustrates how TS-EVs can contribute to extending the knowledge on complex multifactorial diseases, facilitating the development of EV-based diagnostic and therapeutic strategies.

The interest in enriching and characterizing TS-EVs extends beyond the nervous system. There are significant efforts in cancer research, as well as in studies related to pathological processes in major tissues and organs (e.g. liver, lung, prostate and placenta) (Mondal and Whiteside 2021, Brett et al. 2017, Carnino et al. 2019, Miranda et al. 2018, Newman et al. 2022). The present study aimed at developing and validating an immunoaffinity protocol to enrich TS-EVs from human plasma. We established and present an analytical workflow for investigating EVs derived from the nervous system, alveolar type 1 cells, hepatocytes and placental trophoblasts (Figure 1).

2 | Methods

2.1 | Human Plasma Specimens

Multiple pools of human EDTA-K2 plasma from healthy donors (gender pooled) (BioIVT, Westbury, NY) were used to isolate total EVs and EV subpopulations bearing specific antigens. For placenta-derived EVs, we used individual human EDTA-K2 plasma from confirmed pregnant donors (BioIVT, Westbury, NY), while individual plasma samples from non-pregnant healthy female and male volunteers were included as negative controls. Samples were stored at −20°C and thawed on ice before use.

2.2 | EV Enrichment

2.2.1 | Total EV Enrichment

Total EVs were enriched by ultracentrifugation. Briefly, 350 µL of plasma sample was centrifuged at 4°C for 10 min at 300 rcf, after the addition of 150 µL of Tris HCl (pH 7.2) and 1 mL of 0.22 µm-filtered 1X DPBS. The supernatant was transferred to a new tube, then centrifuged at 4°C for 10 min at 2000 rcf, for 30 min at 10,000 rcf and an additional 5 min at 15,000 rcf. The supernatant was then diluted with 0.22 µm-filtered 1X DPBS to a final volume of 12 mL and ultracentrifuged for 120 min at 111,000 rcf by using the rotor 'Type 50.2 Ti' (Optima L-90K, Beckman Coulter, NJ, USA). The resulting pellet was resuspended in 500 µL of Binding Buffer (ExoSORT, Cat. No. Ex-015, Neurodex, Natick, MA, USA) supplemented with Protease and Phosphatase inhibitors 2X (HALT, Cat. No. 78346 and 78429, Thermo Fisher Scientific, Waltham, MA, USA) if intended to be used to enrich TS-EVs by immunoprecipitation protocol, or in 500 µL of 0.22 µm-filtered 1X DPBS if intended to be used as total EVs. Not-lysed total EVs were not treated with Protease and Phosphatase inhibitors since DPBS is inert and does not have any proteolytic and phospholytic activities.

2.2.2 | Biotinylation of Antibodies

Unconjugated antibodies (see Table 1) were biotinylated by adding 13.3 µL of 12.86 mM EZ-Biotin (EZ-Link NHS-SS-PEG4-Biotin, Cat. No. A39259, Thermo Fisher Scientific, Waltham, MA, USA) for each 1 mg/mL of antibody and incubated overnight at 4°C. Buffer exchange was performed using the Zeba Spin Desalting Columns, 7K MWCO (Cat. No. 89877, Thermo Fisher Scientific, Waltham, MA, USA) before the addition of EZ-Biotin (only for antibodies formulated with primary amines), and after the addition of EZ-Biotin to remove its residual, according to the manufacturer's instructions. The incorporation of biotin was verified using immuno-plates with high binding surface (Nunc,

TABLE 1 | Surface protein markers and human primary antibodies used to enrich TS-EVs by immunoaffinity capture.

Surface antigen	Vendor	Antibody Cat. N.	Type	Antibody amount for IP (μg)	Cell of origin	Organ/tissue
GAP43 Growth-associated protein 43	Neurodex, (Natick, MA, USA)	NDXNL3	Monoclonal	5.0	Neuron	NS
NLGN3 Neuroligin 3			Monoclonal		Neuron	NS
GLAST Glutamate Aspartate Transporter	Miltenyi Biotec (Bergisch Gladbach, Germany)	130-118-984	Monoclonal	5.0	Astrocyte	NS
TMEM119* Transmembrane protein 119	Protein Tech (Rosemont, IL, USA)	66948-1-PBS	Monoclonal	5.0	Microglia cell	NS
HT1-56* Human type I cell 56-kDa protein	Terrace Biotech (San Francisco, CA, USA)	TB-29AHT1-56	Monoclonal	2.5	Alveolar Type 1 cell	Lung
AGER Advanced Glycosylation End-Product Specific Receptor	LS-Bio (Shirley, MA, USA)	LSC529077	Monoclonal	2.5	Alveolar Type 1 cell	Lung
ASGPR1 Asialoglycoprotein receptor 1	Novus Biologicals (Centennial, CO, USA)	NBP2-89636B	Monoclonal	5.0	Hepatocyte	Liver
GLUT2 Glucose Transporter 2	Thermo Fisher, (Waltham, MA, USA)	GLUT2-1-BIOTIN	Polyclonal	2.5	Hepatocyte	Liver
PLAP Placental alkaline phosphatase		13-9870-82	Monoclonal	2.5	Placental Trophoblast	Placenta
IgG* Isotype Control		31235	Polyclonal	2.5/5.0	N/A	N/A

*Antibodies biotinylated as described in the Methods paragraph.

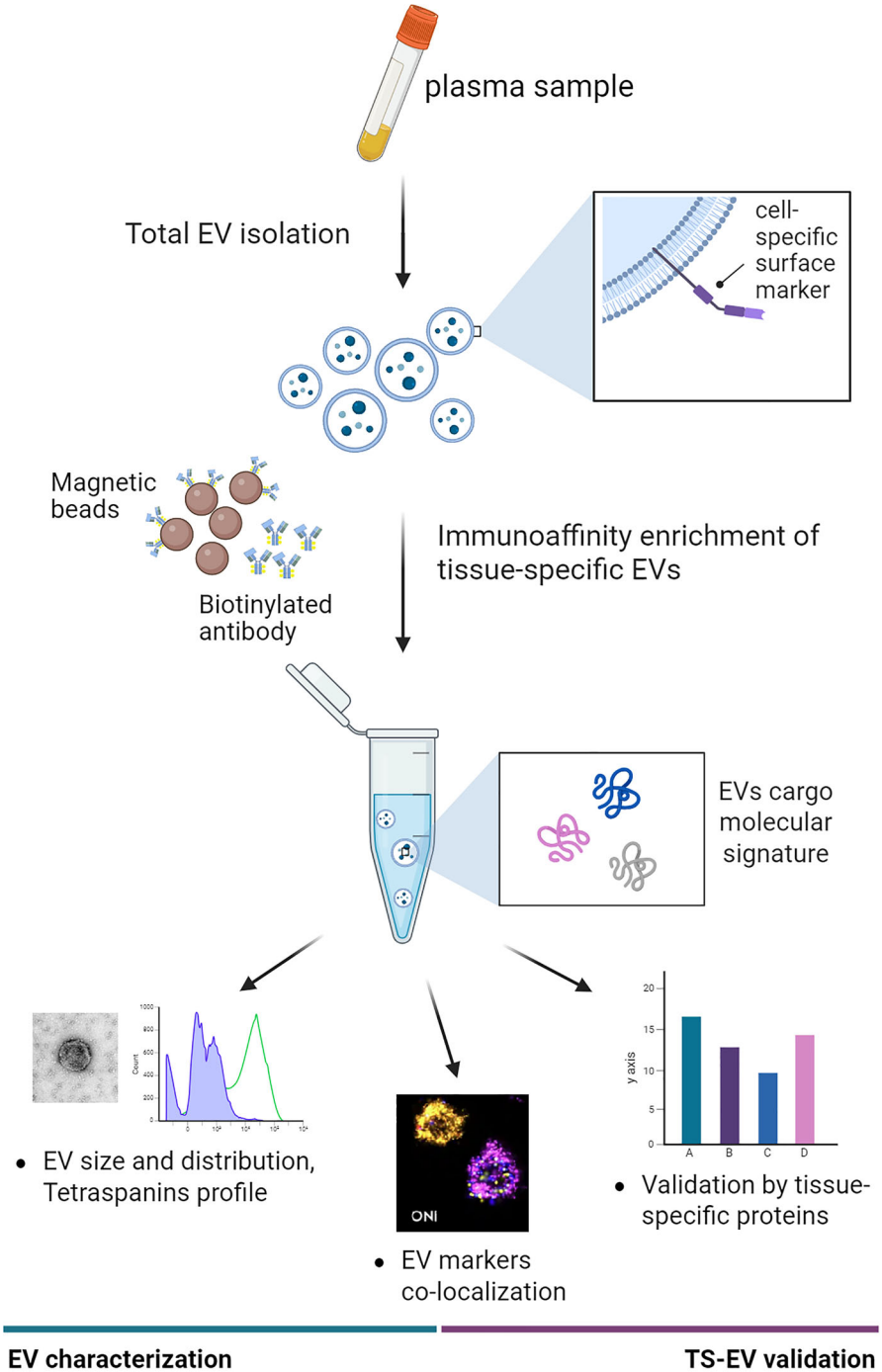

FIGURE 1 | Analytical workflow. TS-EVs are enriched from human plasma specimens through an immunoaffinity protocol targeting cell-specific surface markers and using streptavidin-modified magnetic beads coated with biotinylated antibodies. The subpopulations of TS-EVs are characterized for general EV features such as size, distribution and tetraspanins profile. Tissue-specific markers are co-localized with general EV markers through single EV super resolution imaging. The TS-EV cargo expresses a molecular signature specific to the type of cell/tissue targeted, enabling the assessment of validation protein markers by immunoassays.

Cat. No. 442404, Thermo Fisher Scientific, Waltham, MA, USA), through the reaction with streptavidin-HRP (Bio Legend, Cat. No. 405210, San Diego, CA, USA) and the colorimetric detection with TMB ultrasensitive substrate (Millipore Sigma, Cat. No. ES022, Burlington, MA, USA). The fluorescence was measured at 450 nm by the Synergy H1 microplate reader (Biotek, Winooski, VT, USA).

2.2.3 | Enrichment of TS-EVs by Immunoaffinity Capture

The surface proteins to immunocapture the subpopulations of TS-EVs of interest were selected based on current evidence in literature, when available, or by screening public databases such

as the Human Protein Atlas (HPA) (Uhlén et al. 2015), which reports tissue expression profile at mRNA and protein levels, Uniprot (Consortium et al. 2025), which reports annotation of protein expression and subcellular localization, and Vesiclepedia (Pathan et al. 2019, Chitti et al. 2024), a compendium of molecular data, including proteins, identified in different classes of EVs. We screened and selected surface proteins exclusively or mainly expressed in the cell/tissue type of interest, located on the cell membrane and identified or presumably present on the surface of EVs. If multiple potential surface protein targets were selected, we also performed the immunoaffinity capture using a combination of antibodies in a single reaction, deriving EVs positive for at least one of the two markers (indicated as '||'), or using a sequential capture to derive double-positive EVs for the two markers (indicated as '/').

Enrichment was performed with ExoSORT kit (NeuroDex, Cat. No. NDX_ESNeuro, Natick, MA, USA), with several modifications. Magnetic beads, streptavidin modified (Cat. No. Ex-BS511, ExoSORT NeuroDex) were conjugated with biotinylated antibodies specific to the surface markers of the TS-EV of interest. Antibodies and isotype control (IgG) can be found in Table 1. In detail, 25 µL of magnetic beads per sample were incubated on a rotator with an amount of antibody ranging between 2.5 and 5 µg (depending on the antibody, see Table 1), for 1.5 h at room temperature (RT). Then, the solution was blocked with 5 µL of Blocking Reagent (Cat. No. Ex-012, ExoSORT NeuroDex) for 1 h at RT. The beads were reconstituted in 50 µL of the supplemented Binding Buffer (Cat. No. Ex-015, ExoSORT NeuroDex) and incubated overnight at 4°C with the resuspended pellet obtained from the ultracentrifugation. The following day, using a magnetic separator, all the unconjugated materials (IP unbound) were saved, while the complexes of beads with the immunocaptured-EV were washed three times (ExoSORT Wash Buffer, Cat. No. Ex-016, NeuroDex) and air-dried for 3 min at RT, ensuring complete removal of all liquid. Then, 35 µL of low pH elution buffer (Cat. No. EX-017, ExoSORT NeuroDex) was added and incubated for 5 min at 50°C, allowing the disruption of antibody-antigen interactions, therefore releasing intact immunocaptured EVs from the beads. Eluates were collected using a magnetic separator and transferred into clean tubes, adding 125 µL of lysis buffer (Cat. No. Ex-018, ExoSORT NeuroDex or equivalent Pierce IP Lysis Buffer, Cat. No. 87787, Thermo Fisher Scientific, Waltham, MA, USA), supplemented with Protease and Phosphatase inhibitors 1X, and 5 µL of neutralizing TRIS buffer. Incubated on ice for 20 min, the immunocaptured EVs were stored at −20°C or immediately used for downstream analysis. Total EVs, obtained as described earlier in the method, and the unbound fractions from the immunoaffinity capture, were lysed and stored following the same steps of immunocaptured-EVs. Non-lysed immunocaptured-EVs were stored in elution buffer and neutralizing TRIS buffer for downstream analysis requiring intact membrane, including transmission electron microscopy (TEM), nanoparticle flow cytometry (NanoFCM), super resolution microscopy, and tetraspanins, apolipoproteins, and albumin immunoassay measurements.

2.2.4 | Enrichment of GLUT2$^+$/ASGR1$^+$ EVs by a Sequential Immunoaffinity Capture

The immunoaffinity capture protocol was modified to perform a sequential immunocapture on hepatocyte-derived EVs, targeting the surface markers GLUT2 and ASGR1 in two consecutive steps. As described above, the complex of beads and immunocaptured-EVs obtained from the overnight incubation with the anti-GLUT2 biotinylated antibody (2.5 µg), was washed three times and air-dried for 3 min, and finally eluted in 35 µL of elution buffer. Then, the resulting GLUT2$^+$ EVs were released from magnetic beads and neutralized using 5 µL of Tris HCl pH 7.5 and 150 µL of DPBS. An additional 410 µL of supplemented Binding Buffer was added for a final volume of 600 µL. The samples were then incubated overnight (4°C) with magnetic beads conjugated with the anti-ASGR1 biotinylated antibody (2.5 µg). The following day, the purified GLUT2$^+$/ASGR1$^+$ EVs were washed, dried, eluted, and lysed as described above.

2.2.5 | Total Protein Quantification

Total protein quantification was determined using Qubit Protein Assay (Cat. No. Q33212, Thermo Fisher Scientific, Waltham, MA, USA), according to manufacturer's instructions.

2.3 | EV General Characterization

Non-lysed and freshly prepared immunocaptured-EVs were visualized by TEM at 1:10 dilutions with 0.22 µm-filtered 1X DPBS, as previously described (Comfort et al. 2021), at the Weill Cornell Electron Microscopy & Histology Core Center.

Particle concentration (particle/mL), size distribution and median diameter (nm) were measured on non-lysed EVs using nanoparticle flow cytometry (Flow Nano Analyzer, NanoFCM Co., UK), as previously described (Fabiano et al. 2025), at the EXCEL EV Core at the Johns Hopkins University School of Medicine.

ELISA immunoassays were used for CD81, CD63 and CD9 detection (Cat. No. EXEL-ULTRA-CD81-1, EXEL-ULTRA-CD63-1, EXEL-ULTRA-CD9-1, ExoELISA-ULTRA Complete Kit, System Biosciences, CA, USA). Apolipoprotein A1 (ApoA1) (Cat. No. CSB-E08103h, Cusabio, TX, USA), Apolipoprotein B-100 (ApoB100) (Cat. No. EEL156, Thermo Fisher, MA, USA), Albumin (Cat. No. EHALB, Thermo Fisher, MA, USA), on non-lysed, intact EVs, while Calnexin (Cat. No. LS-F9150, LS-Bio, MA, USA) was measured on lysed EVs. The assays were performed according to manufacturer's instructions and measuring the fluorescence at 450 nm by the Synergy H1 microplate reader (Biotek, Winooski, VT, USA). The standard curve was calculated using a four-parameter logistic curve (4PL).

2.4 | TS-EVs Validation

2.4.1 | Single EV Analysis by dSTORM

Single EV super resolution images were acquired by dSTORM from ONI (Nanoimager S, Oxford Nanoimaging, UK) at the EXCEL EV Core at Johns Hopkins University, School of Medicine. EV Profiler kit 2 was used to visualize and phenotype non-lysed, intact immunocaptured-EVs by analysing three independent channels of fluorescence: Pan-EV and Tetraspanin trio (CD9, CD63, CD81), both provided by the kit, and each tissue-specific surface marker in a third channel. Co-localization analysis was performed with the CODI online analysis platform (https://alto.codi.bio/), with EV profiling settings. Six fields of view were acquired for each sample (five for AGER$^+$ EVs). A modified version of the procedure was applied to the subpopulations of HT1-56$^+$/AGER$^+$ EVs and GLUT2$^+$ || ASGR1$^+$ EVs, labelling each antibody and analysing a single channel per target to increase the sensitivity and assessing the presence of the single proteins or a combination of them, alongside one general EV marker (CD9).

2.4.2 | Immunoassays for Tissue-Specific Markers

The validation protein markers, specific for each intended cell type, were chosen based on the expression of the proteins in the tissue/cell type of interest, and the absence/low expression in those of noninterest. Secreted proteins were excluded, preferentially selecting proteins with cytosolic/lumen subcellular locations and with known involvement in EVs pathways. The detection of these proteins in previous EV studies has been checked using public data repository (Pathan et al. 2019, Chitti et al. 2024). The validation markers were measured on lysed EVs using commercial ELISA kits according to the manufacturers' instructions. Table 2 shows details of the assays performed.

2.4.3 | Statistical Analysis

Total protein concentration was used to normalize the input amount for each tissue-specific target. All experiments were conducted in technical triplicates on five biological replicates (unless otherwise specified). A four-parameter logistic curve (4PL) was applied to analyse ELISA assay results. For some proteins, the expression levels in total EVs were below the detection limit. Thus, we decided to universally normalize the data for each experiment to the immunocaptured EV fractions, which were above the detection limit in all assays. The normalized expression data were then analysed using the Wilcoxon ranked sum test (statistical significance $p < 0.05$). All analyses were conducted in *R* (version 4.2.2).

2.4.4 | EV-Track

All relevant data regarding our methods have been submitted to the EV-TRACK knowledgebase (Van Deun et al. 2017). EV track ID: EV260020 (evtrack.org).

3 | Results

3.1 | General EV Characterization

We enriched EV subpopulations from human plasma by targeting surface proteins expressed by the parental cell and presumably present on the surface of the EVs. We screened cell- and tissue-specific proteins based on recent literature and data available on the HPA public database (Uhlén et al. 2015). Candidate markers were cross-referenced for tissue-specificity, subcellular locations and presence in EV, by using web-based repository such as Uniprot (Consortium et al. 2025) and Vesiclepedia (Chitti et al. 2024). We selected one or more surface targets and validation markers for each cell type and tissue (Figure 2). In situations in which we identified multiple potentially viable antigen targets, we also tested the utility of using a combination of antibodies in a single reaction to derive EVs that were positive for at least one of two markers (e.g. GLUT2$^+$ || ASGR1$^+$), or of using sequential capture to derive double-positive EVs (e.g. GLUT2$^+$/ASGR1$^+$).

We performed a general characterization of the enriched EV subpopulations by NanoFCM and TEM. The immunocaptured-EV subpopulations showed similar size distribution (50–140 nm) and concentration (10^8 particles/mL) to one another (Figure 3A, Table S1). We confirmed typical round or cup-shaped morphology of the particles by TEM, as in the case of GLAST$^+$ EVs, GLUT2$^+$ EVs and GLUT2$^+$/ASGR1$^+$ EVs subpopulations (Figures S1 and S2). Immunocaptured-EV subpopulations showed detectable levels of CD9, CD63, CD81 by ELISA (Figure 3B), about 10 times lower compared to total EVs. CD81 is the most abundant across the TS-EVs, with higher levels detected in GAP43$^+$ || NLGN3$^+$ EVs and AGER$^+$ EVs subpopulation compared to the other immunocaptured-EVs, except for GLUT2$^+$/ASGR1$^+$ EVs, which showed slightly higher CD63 positive EV. The general characterization demonstrated that the subpopulations of immunocaptured-EVs enriched by our workflow had features and canonical markers consistent with those expected for EVs.

Moreover, we evaluated the levels of apolipoproteins and plasma proteins in immunocaptured-EV preparations using immunoassays for ApoA1, ApoB100 and Albumin (Figure 3C–E). As expected, immunocaptured-EV subpopulations showed low levels of both ApoA1 and ApoB100; the average ApoA1 protein concentration across the subpopulations was 536-fold lower than that detected in plasma, while the average ApoB100 concentration in TS-EVs subpopulations was 25-fold lower than the ApoB100 concentration in plasma. Similarly, the average level of Albumin protein across immunocaptured-EVs was ~10^6x lower than the concentration detected in blood plasma. We also measured Calnexin protein by ELISA as an EV negative marker, revealing low levels of this endoplasmic reticulum protein across the subpopulations (Figure 3F). These results confirmed that immunocaptured-EVs enriched by our approach presented low presence of apolipoproteins, plasma proteins or cell components, typically regarded as contamination, being non-EV markers (Brennan et al. 2020, Tóth et al. 2021, Marlęga-Linert et al. 2024).

TABLE 2 | Protein markers and ELISA assays used to validate enriched TS-EVs.

Protein marker	Vendor	Cat. N.	Protein Input (ng)	ELISA detection range (ng/mL)	TS-EV to validate
SYP Human Synaptophysin	CusaBio (Houston, TX, USA)	CSB-E17406h	1000.0–800.0	0.0625–4.0	$GAP43^+$ /$NLGN3^+$ EVs
GFAP Glial fibrillary acidic protein	Thermo Fisher (Waltham, MA, USA)	EEL079	200.0–160.0	0.0156–1.0	$GLAST^+$ EVs
AIF1 Human Allograft Inflammatory Factor 1	CusaBio (Houston, TX, USA)	CSB-El001490HU	500.0–120.0	0.0078–0.5	$TMEM119^+$ EVs
PY12R Purinergic Receptor P2Y12	LS-Bio (Shirley, MA, USA)	LS-F34073	500.0–120.0	0.156–10.0	$TMEM119^+$ EVs
AQP5 Human Aquaporin 5	LS-Bio (Shirley, MA, USA)	LS-F35406	250.0–200.0	0.156–10.0	$HT1\text{-}56^+$ EVs $AGER^+$ EVs $HT1\text{-}56^+$ || $AGER^+$ EVs
NAPSA Human Napsin-A	Ray&Biotech (Peachtree Corners, GA, USA)	ELH-NAPSA	100.0–20.0	0.686–500.0	$HT1\text{-}56^+$ EVs $AGER^+$ EVs $HT1\text{-}56^+$ || $AGER^+$ EVs
CYP2E1 Cytochrome P450 Family 2 Subfamily E Member 1	LS-Bio (Shirley, MA, USA)	LS-F9041	750.0–600.0 500.0–400.0 500.0–400.0 500.0–400.0	0.78–50.0	$GLUT2^+$ EVs $ASGR1^+$ EVs $GLUT2^+$ || $ASGR1^+$ EVs $GLUT2^+$/$ASGR1^+$ EVs
ASGR1/ASGPR Asialoglycoprotein receptor 1	LS-Bio (Shirley, MA, USA)	LS-F4318	1200.0–1000.0 1000.0–800.0 1000.0–800.0 1000.0–800.0	0.156–10.0	$GLUT2^+$ EVs $ASGR1^+$ EVs $GLUT2^+$ || $ASGR1^+$ EVs $GLUT2^+$/$ASGR1^+$ EVs
CYP19A1 Cytochrome P450 family 19 subfamily A member 1	My BioSource (San Diego, CA, USA)	MBS450816	150.0–120.0	0.156–10.0	$PLAP^+$ EVs

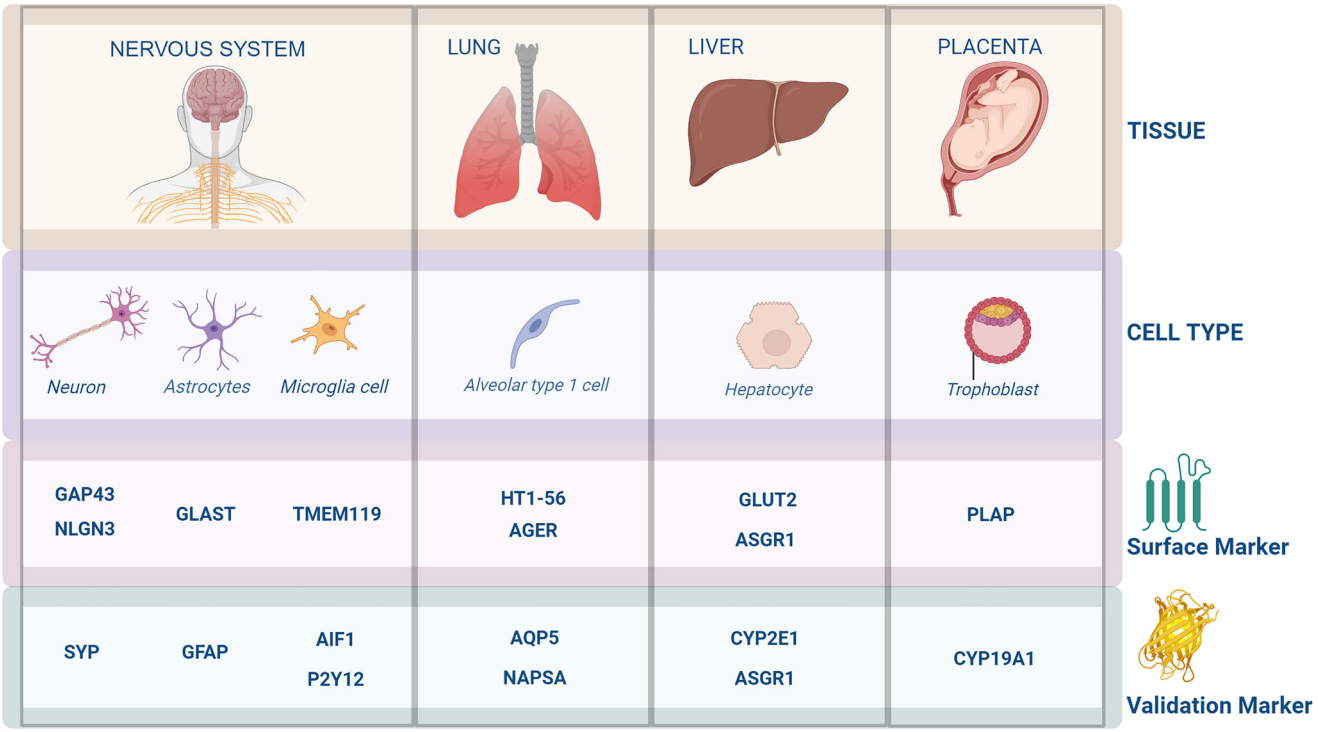

FIGURE 2 | Selection of tissue-specific surface targets and validation markers. Graphic representation of the tissue and cell type explored in this study. Nervous system EVs have been investigated targeting surface markers specific to neurons, astrocytes and microglia cells. The EV subpopulation from neurons was enriched targeting the growth-associated protein 43 (GAP43) and neuroligin 3 (NLGN3) as surface markers, while the validation was assessed by measuring the amount of synaptophysin protein (SYP). EVs released from astrocytes and microglia cells were immunoprecipitated using antibodies towards the glutamate aspartate transporter (GLAST, also known as Excitatory amino acid transporter 1-EAAT1) and the transmembrane protein 119 (TMEM119) respectively and measuring glial fibrillary acidic protein (GFAP) protein for astrocyte EVs, human allograft inflammatory factor 1 (AIF1) and purinergic receptor P2Y12 (P2RY12) for microglia EVs. The human type I cell 56-kDa protein (HT1-56) and/or the advanced glycosylation end-product specific receptor (AGER) were targeted to enrich EVs release from the Alveolar Type 1 lung cells (AT1 cells). The validation was performed by measuring the protein level of human aquaporin 5 (AQP5) and human napsin-A (NAPSA). Liver EVs released from hepatocytes have been immunocaptured targeting glucose transporter 2 (GLUT2) and/or the asialoglycoprotein receptor 1 (ASGR1), validating the protein level of ASGR1 and cytochrome P450 family 2 subfamily E member 1 (CYP2E1). EVs released from the placenta tissue, specifically from trophoblast cells, have been targeted using placental alkaline phosphatase (PLAP) as surface marker, and measuring the level of cytochrome P450 family 19 subfamily A member 1 (CYP19A1) as validation marker.

3.2 | Co-Localization of Canonical and Cell-Specific EV Surface Markers

By detecting single markers on the surface of intact EVs, super resolution microscopy helped us to confirm the surface co-localization of our targeted tissue-specific proteins with EV markers, supporting capture specificity. Tissue/cell-specific surface markers GAP43/NLGN3, GLAST, TMEM119, HT1-56, AGER, GLUT2 and ASGR1 all co-localized with general and canonical EV markers (i.e. Tetraspanins trio, Pan-EV or CD9) (Figure 4). However, we did not observe any co-localization of PLAP, a putative antigen for placental EVs, with any of the EV markers.

3.3 | Validation of Immunocaptured-EVs Measuring the Expression of Cell-Specific Proteins by Immunoassay

For each of the immunocaptured-EV subpopulations, we sought to validate that our method specifically enriches for the intended subpopulation of EVs by the enrichment of tissue-specific luminal or membrane proteins (Figure 5). Additionally, we cross-validated the specificity of our immunocaptured-EVs by using one EV subpopulation ($GLAST^+$ EVs) as control for the others, showing poor enrichment or no detection across different tissue-specific proteins (Figure S3).

3.3.1 | Nervous System—NS EVs

We enriched neuronal EVs using a commercially available mixture of antibodies against the neuronal membrane proteins GAP43 and NLGN3 and validated the capture by measuring the level of the neuronal synaptic marker SYP. We observed that the subpopulation $GAP43^+$ || $NLGN3^+$ EVs from neurons had a ~237-fold enrichment of SYP protein compared to the isotype control ($p = 0.008$), and ~482-fold enrichment compared to total EVs ($p = 0.01$) (Figure 5A). The enrichment was 390x compared to IP unbound fraction ($p = 0.04$) (Figure S4A).

We targeted the transmembrane protein GLAST (also known as Excitatory amino acid transporter 1-EEAT1) to enrich astrocyte

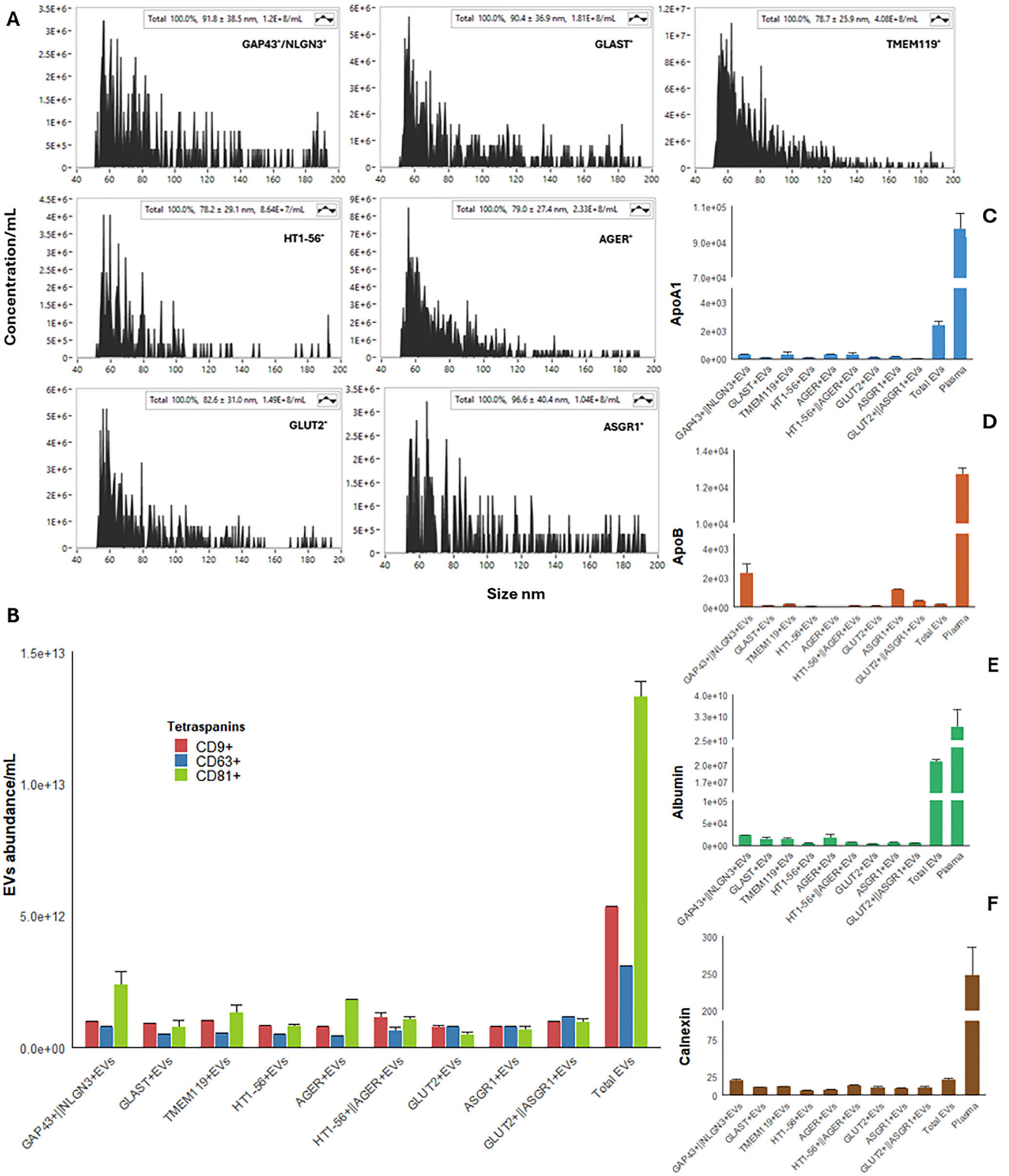

FIGURE 3 | General EV characterization. (A) TS-EV concentration and size distribution. NanoFCM analysis shows the particle number concentration (particles/mL) on the y-axis and the size (diameter) distribution (nm) on the x-axis for each subpopulation of enriched TS-EVs. The box at the top of each plot shows the median values of the particle diameter, ranging from 78.2 ± 29.1 nm to 96.6 nm ± 40.4 nm, and the median values of the concentration, in the range of 10^7–10^8 particles/mL. (B) Tetraspanins profile. Subpopulations of TS-EVs assessed for abundance of EVs positive for CD9, CD63 and CD81 markers (mean ± SEM/mL). (C–F) Apolipoproteins, albumin and calnexin assessment. Subpopulations of TS-EVs, total EVs, and plasma assessed for levels of (C) ApoA1, (D) ApoB100, (E) Albumin and (F) Calnexin proteins (mean concentration ng/mL ± SEM).

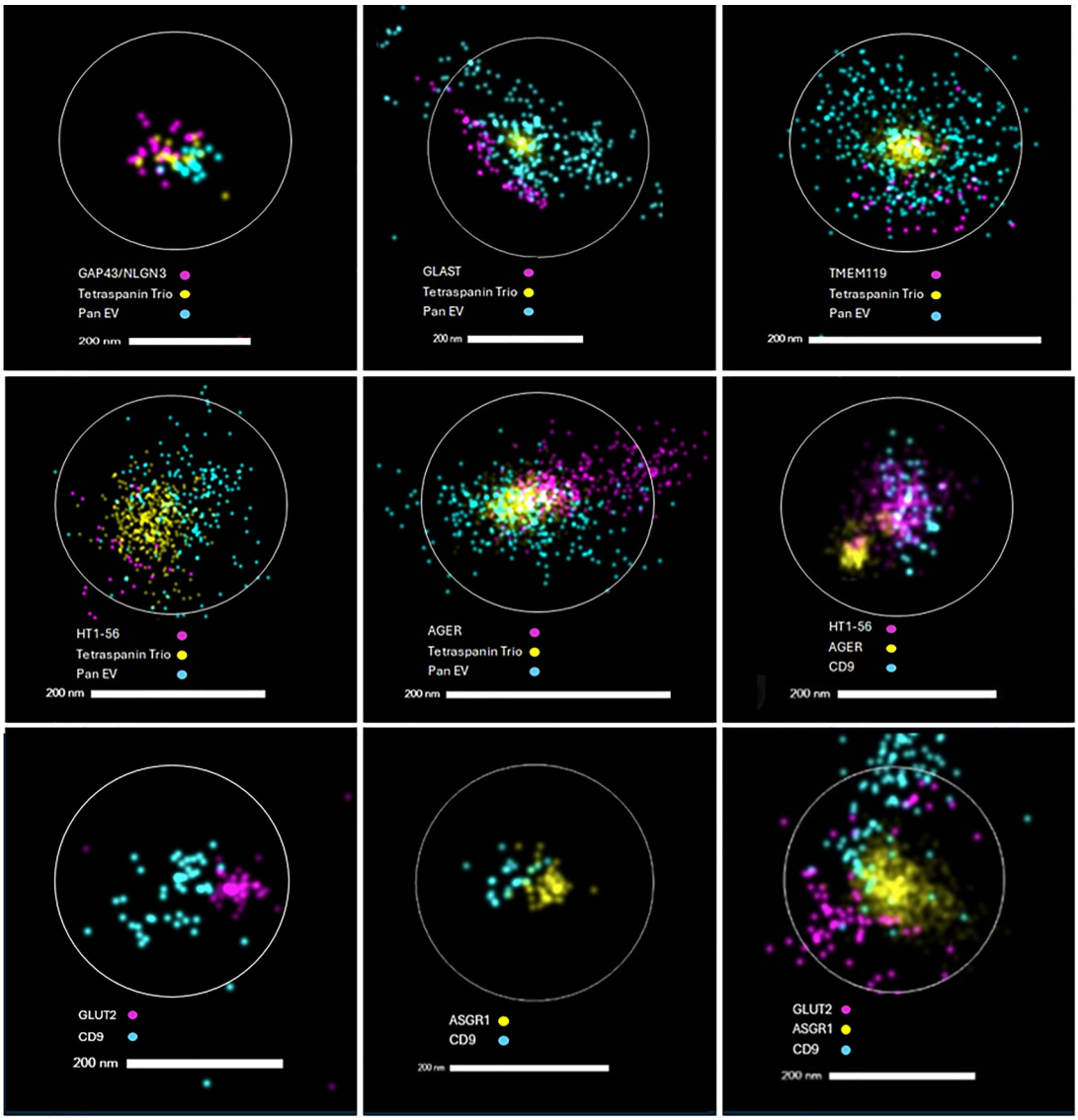

FIGURE 4 | Co-localization of surface markers on single EVs. Single EV analysis by super resolution microscopy shows surface co-localization of tissue-specific and general EV markers (Tetraspanin trio = mixture of CD9, CD63, CD81, 'Pan-EV' stain or CD9 alone) (scale bars 200 nm).

EVs, and we validated the enrichment by the astrocyte marker GFAP. GFAP protein was significantly enriched in the GLAST$^+$ EVs ($p = 0.007$) compared to the IgG, total EV and unbound fraction (Figure 5B, Figure S4B).

We enriched microglia cell-derived EVs targeting the transmembrane protein TMEM119, and we validated the enrichment using two microglial markers, the receptor P2Y12 and the cytosolic/peripheral membrane protein AIF1. The subpopulation TMEM119$^+$ EVs showed a significant enrichment of the P2Y12 ($p = 0.007$), compared to IgG, total EVs, and IP unbound (Figure 5C, Figure S4C). Similarly, AIF1 protein, a sensitive marker for microglial activation, was enriched 23x in TMEM119$^+$ EVs compared to the isotype control ($p = 0.008$), 37x compared to the total EV ($p = 0.008$) (Figure 5D), and 24x compared to the IP unbound fraction ($p = 0.008$) (Figure S4D).

3.3.2 | Alveolar Type 1 Cell EVs

To enrich EVs originating from alveolar type 1 cells, we targeted the cell-specific membrane proteins HT1-56 and AGER. We validated the enrichment by measuring levels of the luminal marker NAPSA and the membrane channel AQP5.

HT1-56$^+$ EVs were enriched 10-fold for NAPSA protein compared to the IgG ($p = 0.008$) and total EVs (not detected, $p = 0.007$) (Figure 5E). The same subpopulation revealed a significant enrichment for the AQP5 marker compared to the IgG isotype control (not detected, $p = 0.007$) and total EV (not detected, $p = 0.007$) (Figure 5H). The enrichment was also significant when compared to the IP unbound fractions ($p < 0.001$) (Figure S4E,F).

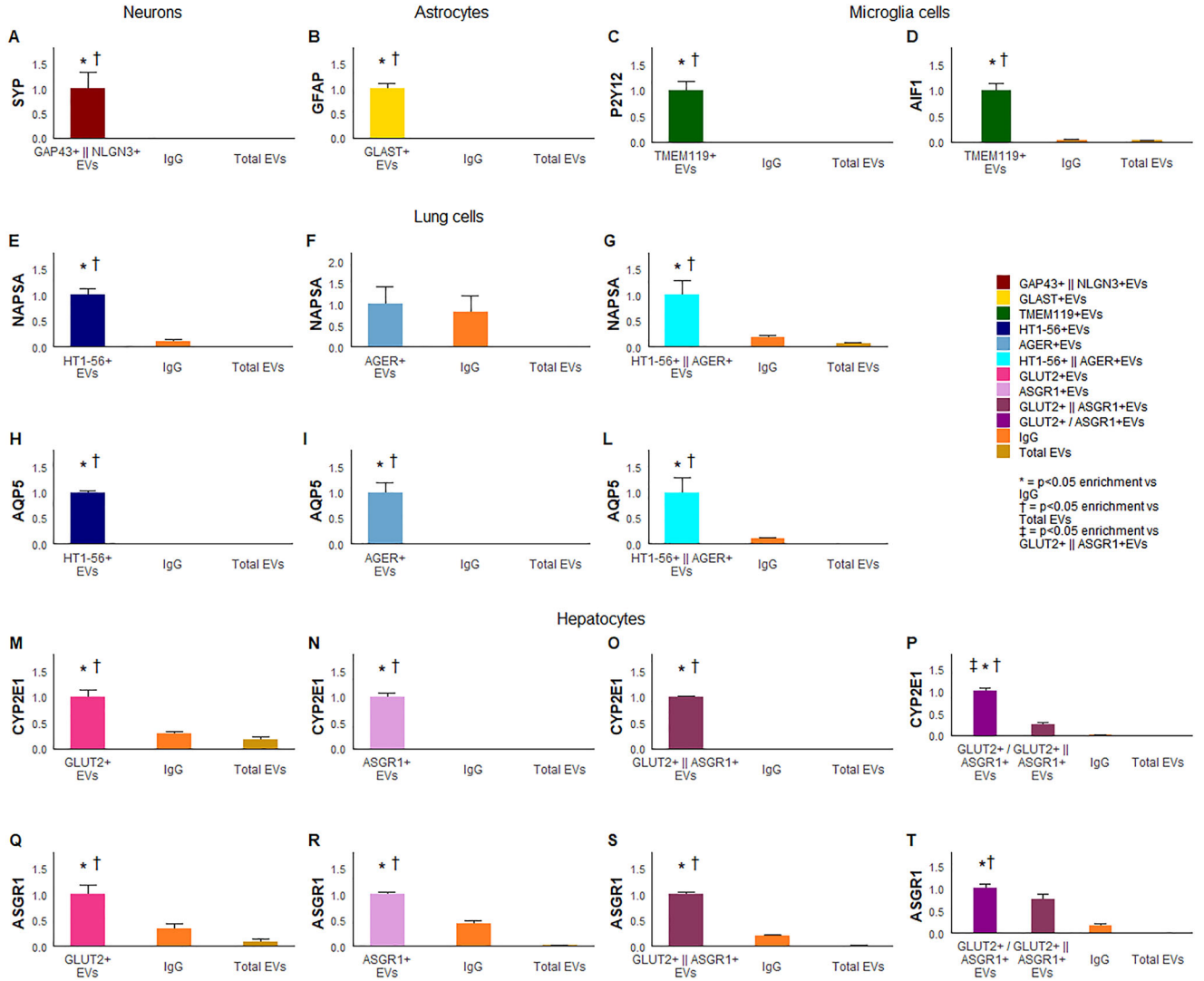

FIGURE 5 | TS-EV validation by immunoassay. Bar plots show EV subpopulations validated for tissue-specific markers, comparing the fractions obtained by IP to the isotype control and the total EV. Data are reported as relative average concentration (ng/mL) ± SEM. (A) GAP43$^+$ || NLGN3$^+$ EVs from neurons; (B) GLAST$^+$ EVs from astrocytes; (C, D) TMEM119$^+$ EVs from microglia cells; (E–H) HT1-56$^+$ EVs, (F–I) AGER$^+$ EVs and (G–L) HT1-56$^+$ || AGER$^+$ EVs from alveolar type I lung cells; (M–Q) GLUT2$^+$ EVs, (N–R) ASGR1$^+$ EVs, (O–S) GLUT2$^+$ || ASGR1$^+$ EVs (positive for at least one marker) and (P–T) GLUT2$^+$/ASGR1$^+$ ('double-positive') EVs from hepatocytes.

The AGER$^+$ EVs did not show any significant enrichment of NAPSA compared to IgG (p = 0.31), while it was significant compared to total EVs (undetected, $p = 0.007$) (Figure 5F, Figure S4G). AGER$^+$ EVs also showed significant enrichment of AQP5 when compared to IgG ($p = 0.007$), total EVs ($p = 0.007$) and the IP unbound fraction ($p < 0.001$) (Figure 5I, Figure S4H).

Given that both HT1-56$^+$ and AGER$^+$ were potential targets for alveolar EV enrichment, we tested the utility of using both antibodies simultaneously in a single immunocapture step. The HT1-56$^+$ || AGER$^+$ population (i.e. EVs positive for at least one of the two markers) showed a 5.4-fold enrichment in NAPSA compared to IgG ($p = 0.01$), and 13.8-fold compared to total EVs ($p = 0.007$) (Figure 5G). For AQP5, HT1-56$^+$ || AGER$^+$ EVs showed significant enrichment compared to IgG (10.2-fold, $p = 0.008$) and total EV (undetected, $p = 0.007$) (Figure 5L). Overall, it appears that most of the enrichment in this process was driven by HT1-56$^+$ EVs, and that the combination of both antibodies did not substantially improve the enrichment.

3.3.3 | Hepatocyte EVs

We tested GLUT2 and ASGR1, two transmembrane proteins highly expressed in hepatocytes, as potential targets for the enrichment of hepatocyte-derived EVs. We validated the enrichment by measuring levels of the liver markers CYP2E1 and ASGR1.

GLUT2$^+$ EVs showed 3.3-fold enrichment in CYP2E1 protein compared to the isotype control ($p = 0.008$) and 5.4-fold compared to total EV ($p = 0.008$) (Figure 4M). GLUT2$^+$ EVs also showed a 3-fold enrichment for the ASGR1 marker compared to IgG ($p = 0.01$) and 13.8-fold enrichment compared to total EV ($p = 0.01$) (Figure 5Q). GLUT2$^+$ EVs were also significantly enriched in both

CYP2E1 ($p = 0.005$) and ASGR1 ($p = 0.004$) compared to the unbound fractions (Figure S4K,L).

Similarly, the ASGR1$^+$ EVs showed a significant enrichment for CYP2E1 protein compared to IgG and total EV (both undetected, $p = 0.007$) (Figure 5N). The ASGR1$^+$ EVs also showed 2.3-fold enrichment for the ASGR1 marker when compared to IgG ($p = 0.008$) and 43-fold compared to total EVs ($p = 0.008$) (Figure 5R). ASGR1$^+$ EVs were also enriched for CYP2E1 and ASGR1 compared to the unbound fractions ($p < 0.001$) (Figure S4M,N).

Given that both GLUT2$^+$ and ASGR1$^+$ showed promise for hepatocyte EV enrichment, we tested the utility of using both antibodies simultaneously in a single immunocapture step to derive EVs positive for at least one of GLUT2 or ASGR1. These GLUT2$^+$ || ASGR1$^+$ EVs showed ~272-fold enrichment of CYP2E1 compared to the IgG ($p = 0.01$) and a significant enrichment compared to the total EVs ($p = 0.007$) (Figure 5O). This simultaneous approach also showed a 5-fold enrichment of the ASGR1 marker levels compared to IgG ($p = 0.008$), 97-fold enrichment compared to total EV ($p = 0.008$) (Figure 5S), and significant enrichment compared to the unbound fractions ($p < 0.001$) (Figure S4O,P). Overall, the simultaneous use of the targets slightly improved the enrichment when compared to the single-positive capture.

While GLUT2 and ASGR1 are most highly expressed in the liver, GLUT2 protein is also expressed in the digestive tract and kidney, while ASGR1 is also expressed in the stomach and gallbladder. Thus, to increase the specificity of the immunocapture for hepatocyte-derived EVs, we also performed a sequential enrichment targeting GLUT2 and ASGR1 proteins in two consecutive steps (Figure 5P,T). The resulting subpopulation of double-positive GLUT2$^+$/ASGR1$^+$ EVs presented a 4.2x enrichment of the CYP2E1 protein compared to EVs that were positive for either GLUT2 or ASGR1 ($p = 0.01$). There was also a marginal (1.3x) improvement in the enrichment of ASGR1 protein levels among double-positive GLUT2$^+$/ASGR1$^+$ EVs compared to EVs positive for either GLUT2 or ASGR1 ($p = 0.28$). Thus, our evidence suggests that sequential immunocapture, yielding double-positive EVs, more specifically enriches hepatocyte-derived EVs than capturing single-positive EVs or a mixture of GLUT2$^+$ and ASGR1$^+$ EVs.

3.3.4 | Placental Trophoblast EVs

We tested PLAP as a target for the enrichment of placental trophoblast-derived EVs using blood from pregnant individuals. Consistent with the lack of co-localization between PLAP and canonical EV markers as seen by the single EV microscopy, PLAP$^+$ EVs did not show a significant enrichment of CYP19A1 protein compared to the male control, and non-pregnant female controls (Figure S5). Similar results were shown by using ERW-1$^+$ EVs and measuring CYP19A1 protein (Figure S6).

4 | Discussion

The lack of standardized and reproducible methods has limited the study of TS-EVs. An appropriate and robust enrichment protocol is likely a precondition to successful EV clinical studies (Gao et al. 2023), including biomarker discovery and EV-based liquid biopsy applications. Here, we optimized and extended existing approaches to enrich subpopulations of EVs from circulation, starting from a relatively small volume of frozen plasma, making them suitable for human studies in which biospecimen volumes are often limited. To our knowledge, this is the first method paper that describes a systematic characterization and validation of EV subpopulations derived from lung alveolar cells, hepatocytes and placental trophoblasts, while being compliant with MISEV guidelines. We introduced a key improvement, sequential immunocapture, that improves capture specificity by leveraging two or more proteins that, on their own, may not be exclusively specific to the cell type of origin. Additionally, we expanded on the existing evidence for nervous system cell-derived EVs and established a rigorous, MISEV guideline (Théry et al. 2018, Welsh et al. 2024) informed validation workflow that provides robust evidence for the cell of origin, such as for microglial and astrocyte EVs, which previously lacked systematic validation.

To our knowledge, this is the first paper enriching and validating lung alveolar type I cell EVs from human blood plasma. EVs released from pulmonary tissue have been mainly investigated through in vitro models of lung disease (Feng et al. 2021, Hu et al. 2022, Akbar et al. 2022) and recently collected from human exhaled breath condensate (Mitchell et al. 2024). The exhaled breath condensates carry markers specific to club cells and alveolar type II cells. In contrast, our approach from blood plasma focused on alveolar type I cells that cover most of the internal surface area of the lung alveoli (~70%) and are commonly damaged in acute and chronic lung diseases. Lung injuries, like chronic obstructive pulmonary disease (COPD), can contribute to altered release and content of lung-derived EVs (Bartel et al. 2024); therefore, EVs originating from type 1 cells can be representative of the overall condition of the lung tissue, especially in active damage. Our results showed that the EV subpopulation expressing the protein HT1-56, an integral membrane protein specific to human alveolar type I cells (Dobbs et al. 1999), presented high levels of NAPSA and AQP5. NAPSA is an aspartic proteinase mainly localized in pneumocytes and alveolar macrophages (Ordóñez 2012), while AQP5 plays a role in alveolar epithelial cell transdifferentiation and alveolar homeostasis (Flodby et al. 2017), and is involved in the progression of lung cancer (Jaskiewicz et al. 2023). The results for AGER, a pro-inflammatory pattern recognition receptor mainly expressed by type I alveolar cells, showed less relative enrichment compared to HT1-56, and the addition of AGER$^+$ antibody to enrich for EVs that were positive for at least one marker (HT1-56$^+$ || AGER$^+$) did not result in meaningfully better specificity. These results may be due to the multiple potential origins of AGER, as it is also expressed at low levels in the brain, adrenal gland and kidney. However, AGER is most highly expressed in lung tissue, and the co-localization pattern of HT1-56 and AGER on the surface of EV does provide additional corroborating evidence that HT1-56 captures EVs of alveolar origin.

Total bloodborne EVs have been studied in the context of liver diseases, such as non-alcoholic fatty liver disease, fibrosis and hepatocellular carcinoma (Muñoz-Hernández et al. 2022, Urban et al. 2019). Unfortunately, most existing data are based on

total EV preparations, which do not distinguish liver-derived EVs from those derived from other cell types. Recently, one group has used ASGR1 to target liver-derived EVs from blood plasma (Newman et al. 2022, Rodrigues et al. 2021). However, the sensitivity and specificity of the immunocapture approach were not reported, and the characterization of the purified ASGR1$^+$ EV population was limited. Here, we showed that the ASGR1$^+$ EVs are significantly enriched for hepatocyte-specific proteins. We also noted that GLUT2, a glucose transporter expressed on the plasma membrane of hepatocytes, is a viable alternative, and targeting both antigens to isolate EVs that are either ASGR1$^+$ or GLUT2$^+$ led to greater enrichment of hepatocyte-derived EVs compared to either antigen alone.

One key consideration is that both ASGR1 and GLUT2 are not exclusively specific to hepatocytes. GLUT2 protein is also expressed in the digestive tract and kidney, while ASGR1 is also expressed in the stomach and gallbladder, and the use of either antibody, or both simultaneously in a mixture, may result in non-specific capture of EVs from other sources. We overcame this non-specificity via sequential immunocapture. As hepatocytes are the only cells that express both GLUT2 and ASGR1, the GLUT2$^+$/ASGR1$^+$ double-positive EVs from sequential immunocapture showed much greater specificity compared to a single immunocapture step using either antibody or a mixture of both. By employing a sequential immunoaffinity approach, the improved specificity may theoretically result in a small reduction in sensitivity and fewer EVs captured from the desired origin. However, the evidence suggests that the double-positive EVs (GLUT2$^+$/ASGR1$^+$ EVs) are likely more specific to hepatocytes compared to EVs that are positive for either GLUT2 or ASGR1 (GLUT2$^+$ || ASGR1$^+$ EVs), which may lead to information more relevant to the liver.

The smaller difference in ASGR1 protein expression between GLUT2$^+$/ASGR1$^+$ double-positive EVs and GLUT2$^+$ || ASGR1$^+$ EVs may be due to the distribution and source of ASGR1 proteins and technical factors. ASGR1 is a single-pass type II membrane protein (isoform H1a), secreted to exert the endocytosis of plasma glycoproteins (isoform H1b). Considering that hepatocytes predominantly express the transmembrane isoform (Liu et al. 2010, Harris et al. 2012), and the majority of the proteins from small EVs are in the membrane, not in the lumen (Zendrini et al. 2022), we can expect that ASGR1 from hepatocyte EVs is almost exclusively membrane-bound, in contrast to the soluble CYP2E1 found exclusively in cytosol/lumen. Therefore, it is possible that the abundance of ASGR1 on the surface of the hepatocyte EVs may obscure the additional specificity of the sequential immunocapture. Furthermore, the specific epitopes of ASGR1 in the membrane may be affected by the lysis step prior to protein measurement, affecting the performance of the assay and the observed relative enrichment. Lastly, the relative abundance of CYP2E1 and ASGR1 in the luminal cargo of EVs may differ by different biogenesis pathways and surface molecular features.

Nervous system EVs have been previously characterized (Eitan et al. 2023, Goetzl et al. 2016, Visconte et al. 2023), but often lacked systematic validation. Our results confirmed the tissue-specificity of GAP43$^+$ || NLGN3$^+$ EVs, GLAST$^+$ EVs and TMEM119$^+$ EVs derived from neurons, astrocytes and microglia cells, respectively. Immunoassays showed high levels of neuronal protein SYP, astrocyte protein GFAP, and microglia proteins P2Y12 and AIF1, for their respective subpopulations, compared to the isotype control, as well as to the IP unbound fraction and total EVs from plasma. Neurons and astrocytes are characterized by known distinct features and properties within the NS. The synaptic protein SYP, as well as the glial astrocyte marker GFAP, which discerns astrocytes from other glial cells, allowed us to validate the enrichment of the TS-EVs subtypes, consistent with other independent studies (Eitan et al. 2023, Goetzl et al. 2016). Conversely, microglia cells are the resident macrophages of the nervous system, sharing several markers with other resident macrophages. The two most specific microglia protein markers identified so far are TMEM119 and P2Y12 (Jurga et al. 2020), while AIF-1 can also be detected in macrophages outside the nervous system (Guselnikova et al. 2024). However, AIF-1 is one of the most used cytosolic markers of microglia activation, given the role exerted in the reorganization of microglial cytoskeleton and phagocytosis (Jurga et al. 2020). Consistent with our results, EV released from microglia, detected from murine brain tissue and cerebrospinal fluid, showed a characteristic cargo of TMEM119 and AIF-1 (Brenna et al. 2020, Roseborough et al. 2023).

Our results do not support the use of surface protein PLAP for the enrichment of placental trophoblast EVs from blood plasma. Previous literature reported mixed data regarding the use of this marker to enrich placental EV. PLAP$^+$ EVs have been reported to increase with gestational age in pregnant women (Sarker et al. 2014), but it is also detectable in non-pregnant individuals (Shinde et al. 2024). Some have attributed this non-specificity to a cross-reaction of the placental alkaline phosphatase to different isoforms of the protein, owing to the high homology to other alkaline phosphatases (Sharma et al. 2014). Our results show that CYP19A1 abundance was comparable in EVs derived from blood plasma across pregnant donors, men and non-pregnant donors. Similarly, super resolution imaging of single EVs did not identify any clustering of PLAP with general EV markers. Similar results were obtained by using PLAP antibody from a different vendor (Cat. No. NBP2-76655B, Novus Biologicals). In addition, we tested the protein Syncytin-1 (Cat. No. ERVW1-BIOTIN, Thermo Fisher), previously described to immunophenotype EVs of placental origin by flow cytometry (Ferrari et al. 2022). Our validation on ERVW-1$^+$ EVs did not produce significant enrichment of placental marker compared to controls and other fractions.

The distribution of tetraspanins can vary based on several factors, such as anticoagulants, EV isolation methods and analysis methods (Karimi et al. 2022, Mizenko et al. 2021). Our results show that this distribution can also vary across different EV subpopulations. While for the majority of our immunocaptured-EVs, CD81 is the most abundant tetraspanin, we observed a slightly different pattern for the hepatocyte-derived subpopulations, with CD63 and CD9 as more abundant compared to CD81. Interestingly, CD81 has been observed as a typical tetraspanin expressed by EVs isolated from cerebrospinal fluid and brain tissue, consistent with what we observed on the subpopulations of circulating neuronal-, astrocyte- and microglial EVs (Ferrari et al. 2022). Heterogeneity in tetraspanins distribution was reported between cell lines (Kugeratski et al. 2021, Tordoff et al. 2024), and thus the heterogeneity we observed further supports distinct origin.

By targeting tissue-specific markers expressed on the surface of EVs, our method enables the enrichment of subpopulations of EVs from the intended tissue that are representative of the tissue status. The identification of targetable surface markers specific to the cell/tissue of interest is a fundamental step to specific capture of TS-EVs. It is possible that the markers identified for their high tissue-specificity can be expressed at lower levels in other tissue types, thereby limiting their specificity. The use of multiple surface proteins, as for the lung and the liver subpopulations, enabled us to improve the specific capture of the EV subtypes of interest. One of the key strengths of our study is the use of sequential immunocapture to overcome the non-exclusive specificity of the single targets, deriving double-positive EVs with higher enrichment. Similarly, our study provides full validation data consistent with MISEV guidelines and uses multiple validation markers to recognize the tissue of origin of the EV subpopulations, confirming the reliability of the independent results obtained. As protein expression patterns are routinely used to identify cell types across different applications, including immune cells phenotyping or tissue staining in pathological diagnostic, our workflow can be applied to circulating TS-EVs from other major organs, for which further investigations are needed to define tissue/cell-type specific targetable markers.

As previously stated, the use of a small volume of frozen plasma is an additional value to our workflow and makes it suitable for human studies in which biospecimen volumes are often limited. Due to the relative abundance of each EV subpopulation in circulation, some downstream analysis, such as omics-based method, could require higher input material to appreciate meaningful signals, based on the technology sensitivity. Emerging high sensitivity platforms might be instead feasible with the use of low input material (Zheng et al. 2026).

While we use tissue-specific surface markers to immunocapture EV subpopulations putatively originating from alveolar type 1 cells, hepatocytes and nervous system cells, we acknowledge that these markers do not provide definitive evidence of tissue-of-origin. Rather, our approach enriches for antigen-positive EV populations that are most plausibly derived from these tissues based on the specificity of the selected proteins. This interpretation is consistent with established practices, but we recognize that additional orthogonal evidence would be required for conclusive assignment. While the co-expression of multiple tissue-associated markers on individual EVs cannot be entirely excluded, the use of highly tissue-enriched markers and independent validation with luminal proteins supports the interpretation that the captured populations are enriched for their intended sources. EV populations are inherently heterogeneous, and it is unlikely that all EVs released from a given tissue or cell type uniformly express the same set of surface antigens. As such, our immunocapture strategy likely enrich only a subset of the total EV population originating from each tissue (Pierri et al. 2026). Collectively, these considerations underscore that our approach should be interpreted as enrichment of tissue-associated EV subpopulations rather than definitive isolation of all EVs derived from a given tissue.

A potential limitation of this study is the lack of validation in in vitro or ex vivo systems or the use of multi-marker or omics-based approach. However, substantial evidence indicates that EVs isolated directly from tissue or primary cell cultures substantially differ from EVs released in vivo, where cells exist within a complex three-dimensional environment and must traverse endothelial barriers to enter circulation (Crescitelli et al. 2021, Lee et al. 2024, Xu et al. 2024, Thippabhotla et al. 2019). Consistent with this, we have shown that brain tissue-EVs are larger and exhibit distinct surface charge and protein frequency patterns compared with neuronal EVs enriched from plasma circulation, despite tissue-specific markers overlap (Kalia et al. 2025). These differences highlight the strong influence of physiological context and microenvironment on EV composition and limit the interpretive value of in vitro or ex vivo validation for TS-EVs captured from circulation. Moreover, many commonly used markers, including proteins and small RNAs, are highly tissue-enriched but not tissue-exclusive. As a result, tissue-specificity becomes particularly critical in multi-marker or omics-based analyses, relying on methods that could introduce additional bias and uncertainty.

Another limitation of this study is that, although the super resolution microscopy confirmed the colocalization of tissue-specific and general EV markers on individual EVs, the frequency and distribution of all possible marker combinations were not comprehensively quantified and warrant further investigation.

In summary, our work provides a validated method to enrich subpopulations of alveolar, hepatocyte, and nervous system EVs from blood plasma, facilitating a broad spectrum of EV-based applications. Examining the molecular information contained in subpopulations of EVs allows us to reach difficult-to-access organs, providing insight toward their health or disease phenotype, while avoiding invasive sampling of the tissue, which is often not feasible. The subpopulations of EVs we enriched and validated represent a promising tool for liquid biopsy to elucidate acute or chronic lung and liver conditions. Likewise, the validated subpopulation of microglia-derived EVs, in addition to neuron- and astrocyte–derived EVs, can extend the breadth of EV applications to neurological conditions not yet explored. TS-EVs can represent a breakthrough advancement for translational medicine, from a better understanding of underlying biological mechanisms to clinical and therapeutic applications.

Establishing the validity and the feasibility of our workflow for lung alveolar cells, hepatocytes and nervous system cells, we are opening promising pathways to (i) apply TS-EV-biology to achieve deep understanding of physiological/pathological status of the source tissue, as well as shed light on the role exerted by the messages carried by each EV subpopulation; (ii) explore diagnostic, prognostic, and therapeutic response-monitoring of TS-EV-based biomarkers; and (iii) provide novel instruments and information to progress drug delivery to specific tissues.

Author Contributions

Biancamaria Pierri: conceptualization, methodology, investigation, formal analysis, writing – original draft, data curation. **Gabriela L. Jackson**: data curation, investigation, formal analysis, writing – review and editing. **Olesia Gololobova**: investigation, formal analysis, writing – review and editing. **Fang Wang**: investigation, formal analysis, writing – review and editing. **Erez Eitan**: validation, writing – review and

editing. **Vrinda Kalia**: validation, writing – review and editing. **Louise C. Laurent**: validation, writing – review and editing. **Kenneth W. Witwer**: validation, writing – review and editing. **Andrea A. Baccarelli**: funding acquisition, validation, writing – review and editing. **Haotian Wu**: conceptualization, methodology, supervision, funding acquisition, writing – original draft.

Acknowledgements

The authors acknowledge the technical support of the Weill Cornell Electron Microscopy & Histology Core Center and EXCEL EV Core at Johns Hopkins University School of Medicine.

Funding

This research is supported by the National Institute of Environmental Health Sciences (NIEHS), Grant number 1R35ES031688-01A1.

Ethics Statement

Not applicable.

Conflicts of Interest

Erez Eitan and Olga Volpert are employed at NeuroDex Inc. The other authors declare no conflicts of interest.

Data Availability Statement

The data that support the findings of this study are available from the corresponding author upon reasonable request.

References

Akbar, S., S. Qadri, S. Ashraf, et al. 2022. "Expression of CD91 in Extracellular Vesicles: A Potential Biomarker for the Diagnosis of Non-Small Cell Lung Cancer." *Advances in Cancer Biology – Metastasis* 4: 100046. https://doi.org/10.1016/j.adcanc.2022.100046.

Bartel, S., J. C. Wolters, H. Noor, et al. 2024. "Altered Extracellular Vesicle-Derived Protein and microRNA Signatures in Bronchoalveolar Lavage Fluid From Patients With Chronic Obstructive Pulmonary Disease." *Cells* 13, no. 11: 945. https://doi.org/10.3390/cells13110945.

Brenna, S., H. C. Altmeppen, B. Mohammadi, et al. 2020. "Characterization of Brain-Derived Extracellular Vesicles Reveals Changes in Cellular Origin After Stroke and Enrichment of the Prion Protein With a Potential Role in Cellular Uptake." *Journal of Extracellular Vesicles* 9, no. 1: 1809065. https://doi.org/10.1080/20013078.2020.1809065.

Brennan, K., K. Martin, S. P. FitzGerald, et al. 2020. "A Comparison of Methods for the Isolation and Separation of Extracellular Vesicles From Protein and Lipid Particles in Human Serum." *Scientific Reports* 10, no. 1: 1039. https://doi.org/10.1038/s41598-020-57497-7.

Brett, S. I., F. Lucien, C. Guo, et al. 2017. "Immunoaffinity Based Methods Are Superior to Kits for Purification of Prostate Derived Extracellular Vesicles From Plasma Samples." *Prostate* 77, no. 13: 1335–1343. https://doi.org/10.1002/pros.23393.

Buzas, E. I. 2023. "The Roles of Extracellular Vesicles in the Immune System." *Nature Reviews Immunology* 23, no. 4: 236–250. https://doi.org/10.1038/s41577-022-00763-8.

Carnino, J. M., H. Lee, and Y. Jin. 2019. "Isolation and Characterization of Extracellular Vesicles From Broncho-Alveolar Lavage Fluid: a Review and Comparison of Different Methods." *Respiratory Research* 20, no. 1: 240. https://doi.org/10.1186/s12931-019-1210-z.

Chitti, S. V., S. Gummadi, T. Kang, et al. 2024. "Vesiclepedia 2024: An Extracellular Vesicles and Extracellular Particles Repository." *Nucleic Acids Research* 52, no. D1: D1694–D1698. https://doi.org/10.1093/nar/gkad1007.

Comfort, N., T. R. Bloomquist, A. P. Shephard, et al. 2021. "Isolation and Characterization of Extracellular Vesicles in Saliva of Children With Asthma." *Extracellular Vesicles and Circulating Nucleic Acids* 2, no. 1: 29–48. https://doi.org/10.20517/evcna.2020.09.

Consortium, T. U. P., A. Bateman, M.-J. Martin, et al. 2025. "UniProt: The Universal Protein Knowledgebase in 2025." *Nucleic Acids Research* 53, no. D1: D609–D617. https://doi.org/10.1093/nar/gkae1010.

Crescitelli, R., C. Lässer, and J. Lötvall. 2021. "Isolation and Characterization of Extracellular Vesicle Subpopulations From Tissues." *Nature Protocols* 16, no. 3: 1548–1580. https://doi.org/10.1038/s41596-020-00466-1.

Dobbs, L. G., R. F. Gonzalez, L. Allen, and D. K. Froh. 1999. "HTI56, an Integral Membrane Protein Specific to Human Alveolar Type I Cells." *Journal of Histochemistry and Cytochemistry* 47, no. 2: 129–137. https://doi.org/10.1177/002215549904700202.

Eitan, E., T. Thornton-Wells, K. Elgart, et al. 2023. "Synaptic Proteins in Neuron-Derived Extracellular Vesicles as Biomarkers for Alzheimer's Disease: Novel Methodology and Clinical Proof of Concept." *Extracellular Vesicles and Circulating Nucleic Acids* 4, no. 1: 133–150. https://doi.org/10.20517/evcna.2023.13.

Fabiano, M. P., A. M. Adamczyk, O. A. Gololobova, et al. 2025. "Plasma Extracellular Vesicle Surface-Located GAS6/PROS1 and CD39/CD73 Attenuate Inflammation." *Cell Reports* 44, no. 8: 116096. https://doi.org/10.1016/j.celrep.2025.116096.

Feng, Z., J. Zhou, Y. Liu, et al. 2021. "Epithelium- and Endothelium-Derived Exosomes Regulate the Alveolar Macrophages by Targeting RGS1 Mediated Calcium Signaling-Dependent Immune Response." *Cell Death and Differentiation* 28, no. 7: 2238–2256. https://doi.org/10.1038/s41418-021-00750-x.

Ferrari, L., S. Iodice, L. Cantone, et al. 2022. "Extracellular Vesicles and Their miRNA Contents Counterbalance the Pro-Inflammatory Effect of Air Pollution During Physiological Pregnancy: A Focus on Syncytin-1 Positive Vesicles." *Environment International* 169: 107502. https://doi.org/10.1016/j.envint.2022.107502.

Fiandaca, M. S., D. Kapogiannis, M. Mapstone, et al. 2015. "Identification of Preclinical Alzheimer's Disease by a Profile of Pathogenic Proteins in Neurally Derived Blood Exosomes: A Case-Control Study." *Alzheimers Dement* 11, no. 6: 600. https://doi.org/10.1016/j.jalz.2014.06.008.

Flodby, P., C. Li, Y. Liu, et al. 2017. "Cell-Specific Expression of Aquaporin-5 (Aqp5) in Alveolar Epithelium Is Directed by GATA6/Sp1 via Histone Acetylation." *Scientific Reports* 7, no. 1: 3473. https://doi.org/10.1038/s41598-017-03152-7.

Gao, J., A. Li, J. Hu, L. Feng, L. Liu, and Z. Shen. 2023. "Recent Developments in Isolating Methods for Exosomes." *Frontiers in Bioengineering and Biotechnology* 10: 1100892. https://doi.org/10.3389/fbioe.2022.1100892.

Gardiner, C., D. Di Vizio, S. Sahoo, et al. 2016. "Techniques Used for the Isolation and Characterization of Extracellular Vesicles: Results of a Worldwide Survey." *Journal of Extracellular Vesicles* 5, no. 1: 32945. https://doi.org/10.3402/jev.v5.32945.

Goetzl, E. J., M. Mustapic, D. Kapogiannis, et al. 2016. "Proteins of Plasma Astrocyte-Derived Exosomes in Alzheimer's Disease." *FASEB Journal* 30, no. 11: 3853–3859. https://doi.org/10.1096/fj.201600756R.

Gomes, D. E., and K. W. Witwer. 2022. "L1CAM-Associated Extracellular Vesicles: A Systematic Review of Nomenclature, Sources, Separation, and Characterization." *Journal of Extracellular Biology* 1, no. 3: e35. https://doi.org/10.1002/jex2.35.

Guselnikova, V. V., V. A. Razenkova, O. V. Kirik, et al. 2024. "Detection of Tissue Macrophages in Different Organs Using Antibodies to the Microglial Marker Iba-1." *Doklady Biochemistry and Biophysics* 519, no. 1: 506–511. https://doi.org/10.1134/S160767292470114X.

Hallal, S., Á. Tűzesi, G. E. Grau, M. E. Buckland, and K. L. Alexander. 2022. "Understanding the Extracellular Vesicle Surface for Clinical Molecular Biology." *Journal of Extracellular Vesicles* 11, no. 10: e12260. https://doi.org/10.1002/jev2.12260.

Harris, R. L., C. W. Van Den Berg, and D. J. Bowen. 2012. "ASGR1andASGR2, the Genes That Encode the Asialoglycoprotein Receptor (Ashwell Receptor), Are Expressed in Peripheral Blood Monocytes and Show Interindividual Differences in Transcript Profile." *Molecular Biology International* 2012: 1–10. https://doi.org/10.1155/2012/283974.

Hu, Q., S. Zhang, Y. Yang, et al. 2022. "Extracellular Vesicles in the Pathogenesis and Treatment of Acute Lung Injury." *Military Medical Research* 9, no. 1: 61. https://doi.org/10.1186/s40779-022-00417-9.

Jaskiewicz, L., A. Romaszko-Wojtowicz, A. Doboszynska, and A. Skowronska. 2023. "The Role of Aquaporin 5 (AQP5) in Lung Adenocarcinoma: A Review Article." *Cells* 12, no. 3: 468. https://doi.org/10.3390/cells12030468.

Jiang, C., F. Hopfner, A. Katsikoudi, et al. 2020. "Serum Neuronal Exosomes Predict and Differentiate Parkinson's Disease From Atypical Parkinsonism." *Journal of Neurology, Neurosurgery, and Psychiatry* 91, no. 7: 720–729. https://doi.org/10.1136/jnnp-2019-322588.

Jurga, A. M., M. Paleczna, and K. Z. Kuter. 2020. "Overview of General and Discriminating Markers of Differential Microglia Phenotypes." *Frontiers in Cellular Neuroscience* 14: 198. https://doi.org/10.3389/fncel.2020.00198.

Kalia, V., G. Jackson, R. J. Dominguez, et al. 2025. "Molecular Profiling of Neuronal Extracellular Vesicles Reveals Brain Tissue Specific Signals." *Exposome* 5, no. 1: p.osaf007. https://doi.org/10.1101/2025.01.23.25320909.

Kalia, V., G. Jackson, R. J. Dominguez, et al. 2025. "Molecular Profiling of Neuronal Extracellular Vesicles Reveals Brain Tissue Specific Signals." *Exposome* 5, no. 1: osaf007. https://doi.org/10.1101/2025.01.23.25320909.

Kalluri, R., and V. S. LeBleu. 2020. "The Biology, Function, and Biomedical Applications of Exosomes." *Science* 367, no. 6478: eaau6977. https://doi.org/10.1126/science.aau6977.

Kalra, H., G. Drummen, and S. Mathivanan. 2016. "Focus on Extracellular Vesicles: Introducing the Next Small Big Thing." *International Journal of Molecular Sciences* 17, no. 2: 170. https://doi.org/10.3390/ijms17020170.

Kapogiannis, D. 2017. "Plasma Extracellular Vesicles Enriched for Neuronal Origin: A Potential Window into Brain Pathologic Processes." *Frontiers in Neuroscience* 11: 278.

Kapogiannis, D., M. Mustapic, M. D. Shardell, et al. 2019. "Association of Extracellular Vesicle Biomarkers With Alzheimer Disease in the Baltimore Longitudinal Study of Aging." *JAMA Neurology* 76, no. 11: 1340. https://doi.org/10.1001/jamaneurol.2019.2462.

Karimi, N., R. Dalirfardouei, T. Dias, J. Lötvall, and C. Lässer. 2022. "Tetraspanins Distinguish Separate Extracellular Vesicle Subpopulations in Human Serum and Plasma—Contributions of Platelet Extracellular Vesicles in Plasma Samples." *Journal of Extracellular Vesicles* 11, no. 5: e12213. https://doi.org/10.1002/jev2.12213.

Kugeratski, F. G., K. Hodge, S. Lilla, et al. 2021. "Quantitative Proteomics Identifies the Core Proteome of Exosomes With Syntenin-1 as the Highest Abundant Protein and a Putative Universal Biomarker." *Nature Cell Biology* 23, no. 6: 631–641. https://doi.org/10.1038/s41556-021-00693-y.

Lee, J. C., R. M. Ray, and T. A. Scott,. 2024. "Prospects and Challenges of Tissue-Derived Extracellular Vesicles." *Molecular Therapy* 32, no. 9: 2950–2978. https://doi.org/10.1016/j.ymthe.2024.06.025.

Li, Y., X. He, Q. Li, et al. 2020. "Enumerating the Tissue-Cellular Origin of Circulating Extracellular Vesicles Using exLR Profile." *Computational and Structural Biotechnology Journal* 18: 2851–2859. https://doi.org/10.1016/j.csbj.2020.10.002.

Liu, J., B. Hu, Y. Yang, et al. 2010. "A New Splice Variant of the Major Subunit of Human Asialoglycoprotein Receptor Encodes a Secreted Form in Hepatocytes." *PLoS ONE* 5, no. 9: e12934. https://doi.org/10.1371/journal.pone.0012934.

Marlęga-Linert, J., A. Gąsecka, E. Van Der Pol, et al. 2024. "Lipoprotein Apheresis Affects the Concentration of Extracellular Vesicles in Patients With Elevated Lipoprotein.(a)." *Scientific Reports* 14, no. 1: 2762. https://doi.org/10.1038/s41598-024-51782-5.

Miranda, J., C. Paules, S. Nair, et al. 2018. "Placental Exosomes Profile in Maternal and Fetal Circulation in Intrauterine Growth Restriction—Liquid Biopsies to Monitoring Fetal Growth." *Placenta* 64: 34–43. https://doi.org/10.1016/j.placenta.2018.02.006.

Mitchell, M. I., I. Z. Ben-Dov, K. Ye, et al. 2024. "Exhaled Breath Condensate Contains Extracellular Vesicles (EVs) That Carry miRNA Cargos of Lung Tissue Origin That Can Be Selectively Purified and Analyzed." *Journal of Extracellular Vesicles* 13, no. 4: e12440. https://doi.org/10.1002/jev2.12440.

Mizenko, R. R., T. Brostoff, T. Rojalin, et al. 2021. "Tetraspanins Are Unevenly Distributed across Single Extracellular Vesicles and Bias Sensitivity to Multiplexed Cancer Biomarkers." *Jornal of Nanobiotechnology* 19, no. 1: 250. https://doi.org/10.1186/s12951-021-00987-1.

Mondal, S. K., and T. L. Whiteside. 2021. "Immunoaffinity-Based Isolation of Melanoma Cell-Derived and T Cell-Derived Exosomes From Plasma of Melanoma Patients." In *Methods in Molecular Biology*, edited by K. M. Melanoma Hargadon, 305–321, Vol. 2265. Springer US. https://doi.org/10.1007/978-1-0716-1205-7_23.

Muñoz-Hernández, R., Á. Rojas, S. Gato, et al. 2022. "Extracellular Vesicles as Biomarkers in Liver Disease." *International Journal of Molecular Sciences* 23, no. 24: 16217. https://doi.org/10.3390/ijms232416217.

Newman, L. A., K. Muller, and A. Rowland. 2022. "Circulating Cell-Specific Extracellular Vesicles as Biomarkers for the Diagnosis and Monitoring of Chronic Liver Diseases." *Cellular and Molecular Life Sciences* 79, no. 5: 232. https://doi.org/10.1007/s00018-022-04256-8.

Newman, L. A., Z. Useckaite, J. Johnson, M. J. Sorich, A. M. Hopkins, and A. Rowland. 2022. "Selective Isolation of Liver-Derived Extracellular Vesicles Redefines Performance of miRNA Biomarkers for Non-Alcoholic Fatty Liver Disease." *Biomedicines* 10, no. 1: 195. https://doi.org/10.3390/biomedicines10010195.

Ordóñez, N. G. 2012. "Napsin A Expression in Lung and Kidney Neoplasia: A Review and Update." *Advances in Anatomic Pathology* 19, no. 1: 66–73. https://doi.org/10.1097/PAP.0b013e31823e472e.

Pathan, M., P. Fonseka, S. V. Chitti, et al. 2019. "A Compendium of RNA, Proteins, Lipids and Metabolites in Extracellular Vesicles." *Nucleic Acids Research* 47, no. D1: D516–D519. https://doi.org/10.1093/nar/gky1029.

Pegtel, D. M., and S. J. E. Gould. 2019. "Exosomes." *Annual Review of Biochemistry* 88, no. 1: 487–514. https://doi.org/10.1146/annurev-biochem-013118-111902.

Picca, A., F. Guerra, R. Calvani, H. Coelho-Junior, C. Bucci, and E. Marzetti. 2022. "Circulating Extracellular Vesicles: Friends and Foes in Neurodegeneration." *Neural Regeneration Research* 17, no. 3: 534. https://doi.org/10.4103/1673-5374.320972.

Pierri, B., E. Eitan, K. W. Witwer, D. B. Re, A. A. Baccarelli, and H. Wu. 2026. "Tissue-Specific Extracellular Vesicles Enriched From Circulation: Exploring the Liquid Biopsy Perspective." *Journal of Extracellular Biology* 5, no. 2: e70106. https://doi.org/10.1002/jex2.70106.

Pulliam, L., B. Sun, M. Mustapic, S. Chawla, and D. Kapogiannis. 2019. "Plasma Neuronal Exosomes Serve as Biomarkers of Cognitive Impairment in HIV Infection and Alzheimer's Disease." *Journal of Neurovirology* 25, no. 5: 702–709. https://doi.org/10.1007/s13365-018-0695-4.

Raposo, G., and W. Stoorvogel. 2013. "Extracellular Vesicles: Exosomes, Microvesicles, and Friends." *Journal of Cell Biology* 200, no. 4: 373–383. https://doi.org/10.1083/jcb.201211138.

Rodrigues, A. D., M. Van Dyk, M. J. Sorich, et al. 2021. "Exploring the Use of Serum-Derived Small Extracellular Vesicles as Liquid Biopsy to Study the Induction of Hepatic Cytochromes P450 and Organic Anion Transporting Polypeptides." *Clinical Pharmacology & Therapeutics* 110, no. 1: 248–258. https://doi.org/10.1002/cpt.2244.

Roseborough, A. D., S. J. Myers, R. Khazaee, et al. 2023. "Plasma Derived Extracellular Vesicle Biomarkers of Microglia Activation in an Experimental Stroke Model." *Journal of Neuroinflammation* 20, no. 1: 20. https://doi.org/10.1186/s12974-023-02708-x.

Sarker, S., K. Scholz-Romero, A. Perez, et al. 2014. "Placenta-Derived Exosomes Continuously Increase in Maternal Circulation over the First Trimester of Pregnancy." *Journal of Translational Medicine* 12, no. 1: 204. https://doi.org/10.1186/1479-5876-12-204.

Sharma, U., D. Pal, and R. Prasad. 2014. "Alkaline Phosphatase: An Overview." *Indian Journal of Clinical Biochemistry* 29, no. 3: 269–278. https://doi.org/10.1007/s12291-013-0408-y.

Shi, M., C. Liu, T. J. Cook, et al. 2014. "Plasma Exosomal α-Synuclein Is Likely CNS-Derived and Increased in Parkinson's Disease." *Acta Neuropathologica* 128, no. 5: 639–650. https://doi.org/10.1007/s00401-014-1314-y.

Shinde, U., A. Rao, V. Bansal, D. K. Das, N. H. Balasinor, and T. Madan. 2024. "Isolation of Serum-Derived Placental/Amnio-Chorionic Extracellular Vesicles across Pregnancy by Immunoaffinity Using PLAP and HLA-G." *Reproduction* 167, no. 4: e230215. https://doi.org/10.1530/REP-23-0215.

Stam, J., S. Bartel, R. Bischoff, and J. C. Wolters. 2021. "Isolation of Extracellular Vesicles With Combined Enrichment Methods." *Journal of Chromatography B* 1169: 122604. https://doi.org/10.1016/j.jchromb.2021.122604.

Ter-Ovanesyan, D., S. Whiteman, T. Gilboa, et al. 2024. "Identification of Markers for the Isolation of Neuron-Specific Extracellular Vesicles." *BioRxiv* 2024. https://doi.org/10.1101/2024.04.03.587267.

Théry, C., K. W. Witwer, E. Aikawa, et al. 2018. "Minimal Information for Studies of Extracellular Vesicles 2018 (MISEV2018): A Position Statement of the International Society for Extracellular Vesicles and Update of the MISEV2014 Guidelines." *Journal of Extracellular Vesicles* 7, no. 1: 1535750. https://doi.org/10.1080/20013078.2018.1535750.

Thippabhotla, S., C. Zhong, and M. He. 2019. "3D Cell Culture Stimulates the Secretion of in Vivo like Extracellular Vesicles." *Scientific Reports* 9, no. 1: 13012. https://doi.org/10.1038/s41598-019-49671-3.

Tordoff, E., J. Allen, K. Elgart, et al. 2024. "A Novel Multiplexed Immunoassay for Surface-Exposed Proteins in Plasma Extracellular Vesicles." *Journal of Extracellular Vesicles* 13, no. 11: e70007. https://doi.org/10.1002/jev2.70007.

Tóth, E. Á., L. Turiák, T. Visnovitz, et al. 2021. "Formation of a Protein Corona on the Surface of Extracellular Vesicles in Blood Plasma." *Journal of Extracellular Vesicles* 10, no. 11: e12140. https://doi.org/10.1002/jev2.12140.

Uhlén, M., L. Fagerberg, B. M. Hallström, et al. 2015. "Proteomics. Tissue-Based Map of the Human Proteome. Science." *Science* 347, no. 6220: 1260419. https://doi.org/10.1126/science.1260419.

Urban, S., T. Mocan, H. Sänger, V. Lukacs-Kornek, and M. Kornek. 2019. "Extracellular Vesicles in Liver Diseases: Diagnostic, Prognostic, and Therapeutic Application." *Seminars in Liver Disease* 39, no. 01: 070–077. https://doi.org/10.1055/s-0038-1676122.

Van Deun, J., P. Mestdagh, P. Agostinis, et al. 2017. "EV-TRACK: Transparent Reporting and Centralizing Knowledge in Extracellular Vesicle Research." *Nature Methods* 14, no. 3: 228–232. https://doi.org/10.1038/nmeth.4185.

Visconte, C., M. T. Golia, C. Fenoglio, et al. 2023. "Plasma Microglial-Derived Extracellular Vesicles Are Increased in Frail Patients With Mild Cognitive Impairment and Exert a Neurotoxic Effect." *GeroScience* 45, no. 3: 1557–1571. https://doi.org/10.1007/s11357-023-00746-0.

Welsh, J. A., D. C. I Goberdhan., L. O'Driscoll, E. I. Buzas, C. Blenkiron, and K. W. Witwer. 2024. "Minimal Information for Studies of Extracellular Vesicles (MISEV2023): From Basic to Advanced Approaches." *Journal of Extracellular Vesicles* 13, no. 2: e12404. https://doi.org/10.1002/jev2.12404.

Wiklander, O. P. B., M. Á. Brennan, J. Lötvall, X. O. Breakefield, and S. El Andaloussi. 2019. "Advances in Therapeutic Applications of Extracellular Vesicles." *Science Translational Medicine* 11, no. 492: eaav8521. https://doi.org/10.1126/scitranslmed.aav8521.

Winston, C. N., E. J. Goetzl, J. C. Akers, et al. 2016. "Prediction of Conversion From Mild Cognitive Impairment to Dementia With Neuronally Derived Blood Exosome Protein Profile." *Alzheimer's & Dementia: Diagnosis, Assessment & Disease Monitoring* 3, no. 1: 63–72. https://doi.org/10.1016/j.dadm.2016.04.001.

Xu, Z., J. B. Foster, R. Lashley, et al. 2024. "Comparison of the Protein Composition of Isolated Extracellular Vesicles From Mouse Brain and Dissociated Brain Cell Culture Medium." *PLoS ONE* 19, no. 11: e0309716. https://doi.org/10.1371/journal.pone.0309716.

Yáñez-Mó, M., P. R. M. Siljander, Z. Andreu, et al. 2015. "Biological Properties of Extracellular Vesicles and Their Physiological Functions." *Journal of Extracellular Vesicles* 4, no. 1: 27066. https://doi.org/10.3402/jev.v4.27066.

You, Y., Z. Zhang, N. Sultana, et al. 2023. "ATP1A3 as a Target for Isolating Neuron-Specific Extracellular Vesicles From Human Brain and Biofluids." *Science Advances* 9, no. 37: eadi3647. https://doi.org/10.1126/sciadv.adi3647.

Yu, D., Y. Li, M. Wang, et al. 2022. "Exosomes as a New Frontier of Cancer Liquid Biopsy." *Molecular Cancer* 21, no. 1: 56. https://doi.org/10.1186/s12943-022-01509-9.

Zarovni, N., D. Mladenović, D. Brambilla, F. Panico, and M. Chiari. 2025. "Stoichiometric Constraints for Detection of EV-borne Biomarkers in Blood." *Journal of Extracellular Vesicles* 14, no. 2: e70034. https://doi.org/10.1002/jev2.70034.

Zendrini, A., G. Guerra, K. Sagini, T. Vagner, D. Di Vizio, and P. Bergese. 2022. "On the Surface-to-Bulk Partition of Proteins in Extracellular Vesicles." *Colloids and Surfaces B: Biointerfaces* 218: 112728. https://doi.org/10.1016/j.colsurfb.2022.112728.

Zheng, W., Y. Jiang, H. Y. Wong, et al. 2026. "Targeted Blood Proteome Profiling Using NULISAseq Identifies a High-Performance Biomarker Panel for Aβ Pathology Quantification and Staging." *Alzheimers Dement* 22, no. 2: e71179. https://doi.org/10.1002/alz.71179.

Supporting Information

Additional supporting information can be found online in the Supporting Information section.

Supporting Information: jex270171-sup-0001-SuppMat.docx